

Efficient Evaluation of the Partition Function of RBMs with Annealed Importance Sampling

Ferran Mazzanti and Enrique Romero

Abstract— Probabilistic models based on Restricted Boltzmann Machines (RBMs) imply the evaluation of normalized Boltzmann factors, which in turn require from the evaluation of the partition function Z . The exact evaluation of Z , though, becomes a forbiddingly expensive task as the system size increases. This even worsens when one considers most usual learning algorithms for RBMs, where the exact evaluation of the gradient of the log-likelihood of the empirical distribution of the data includes the computation of Z at each iteration. The Annealed Importance Sampling (AIS) method provides a tool to stochastically estimate the partition function of the system. So far, the standard use of the AIS algorithm in the Machine Learning context has been done using a large number of Monte Carlo steps. In this work we show that this may not be required if a proper starting probability distribution is employed as the initialization of the AIS algorithm. We analyze the performance of AIS in both small- and large-sized problems, and show that in both cases a good estimation of Z can be obtained with little computational cost.

I. INTRODUCTION

Restricted Boltzmann Machines (RBMs) [1]), constitute a simple variant of the Boltzmann Machines (BM), where connections between units in the same layer are forbidden. This constrain on the topological architecture of the network allows performing calculations in a much more efficient way. However, it still presents the serious drawback of having to evaluate the normalization constant of the resulting probability distribution, called the partition function

$$Z = \sum_{\mathbf{x}, \mathbf{h}} e^{-E(\mathbf{x}, \mathbf{h})}, \quad (1)$$

with $E(\mathbf{x}, \mathbf{h})$ the energy of the different system configurations. In this expression, the sum runs over all possible states, which is an exponential function on the number of units. For this reason, the use of RBMs to build probabilistic models has been marginal, even being one of the key components of the renaissance of deep neural network models at the beginning of the 21th century [2], [3].

The evaluation of the partition function is a required step in learning models based on gradient-descent techniques applied to the log-likelihood of the data. To make things worse, in principle it must be reevaluated at each iteration of the learning process, because the weights setting the strength of correlations between units change. In order to overcome this problem different approximations have been devised, none of

them trying to evaluate Z . The most celebrated choice is the Contrastive Divergence (CD_k) algorithm [4], where all the statistical averages involving Z are replaced by a single sampling reconstructed after k Gibbs sampling steps. Another approach uses Parallel Tempering [5] to generate suitable samples, which allow to estimate the required quantities during the learning process [6]. However, this mechanism may require a large amount of intermediate temperatures, which leads to a large increase in computational cost.

In fact, the partition function Z is a capital quantity appearing in many different fields of science. For instance in physics it yields the Helmholtz free energy, which in turn determines completely the thermodynamic properties of the system. In this way, it is of fundamental interest to be able to find good approximations of it. Among the several possible alternatives [7]–[9], in this paper we focus on the approach developed by R. Neal [10], [11], where an intractable probability distribution is sampled through a random walk on a space of intermediate probability distributions. This algorithm turns out to be efficient in the particular case of the RBM, since the random walk exploration of the intermediate states can be performed by means of Gibbs sampling, which is fully parallelizable [12]. For this reason, the AIS algorithm is the most widely used in the context of RBMs when an estimate of the partition function is required [12]–[18]. However, in most cases the use of AIS becomes computationally expensive since many large chains of intermediate probability distributions are used.

In this paper we show that the AIS algorithm can in fact be used to produce reliable estimates of Z with a small computational cost, even in realistically large problems, when a proper choice of the starting probability distribution is suitably selected. This probability distribution can be built from the weights of the RBM alone, without the need of a training set. We explore different approaches to construct this probability distribution, and test them in different exactly solvable problems. Finally, we compare the results obtained for realistically large problems with those one gets when using the by now standard procedure of Ref. [12].

II. THE PARTITION FUNCTION OF THE RESTRICTED BOLTZMANN MACHINE

The energy function of a binary RBM with N_v visible units \mathbf{x} and N_h hidden units \mathbf{h} , is defined as:

$$E(\mathbf{x}, \mathbf{h}) = -\mathbf{b}^T \mathbf{x} - \mathbf{c}^T \mathbf{h} - \mathbf{x}^T \mathbf{W} \mathbf{h}. \quad (2)$$

This expression can be cast as a quadratic form, where visible and hidden units are organized as row and column vectors

Ferran Mazzanti is with the Departament de Física, Universitat Politècnica de Catalunya - BarcelonaTech, Spain (email: ferran.mazzanti@upc.edu)

Enrique Romero is with the Departament de Ciències de la Computació, Universitat Politècnica de Catalunya - BarcelonaTech, Spain (email: eromero@cs.upc.edu)

preceded by a constant value of 1 to account for the bias terms

$$\tilde{\mathbf{x}} = (1 x_1 x_2 \cdots x_{N_v}) \quad , \quad \tilde{\mathbf{h}} = (1 h_1 h_2 \cdots h_{N_h}) \quad , \quad (3)$$

leading to

$$E(\tilde{\mathbf{x}}, \tilde{\mathbf{h}}) = \tilde{\mathbf{x}}^T \begin{pmatrix} 0 & \mathbf{c} \\ \mathbf{b}^T & \mathbf{W} \end{pmatrix} \tilde{\mathbf{h}} \equiv \tilde{\mathbf{x}}^T \tilde{\mathbf{W}} \tilde{\mathbf{h}} \quad , \quad (4)$$

where $\tilde{\mathbf{W}}$ is the *extended* weights matrix, which includes the bias terms.

As usual in energy-based models, the probability of a state (\mathbf{x}, \mathbf{h}) is

$$P(\mathbf{x}, \mathbf{h}) = \frac{e^{-E(\mathbf{x}, \mathbf{h})}}{Z} \quad , \quad (5)$$

where the normalization term Z is called the partition function

$$Z = \sum_{\mathbf{x}, \mathbf{h}} e^{-E(\mathbf{x}, \mathbf{h})} \quad . \quad (6)$$

The particular form of the energy function (2) makes both $P(\mathbf{h}|\mathbf{x})$ and $P(\mathbf{x}|\mathbf{h})$ to factorize, and so it is possible to compute them in one step. As a consequence, Gibbs sampling can be computed efficiently [19]. In addition, it is also possible to compute efficiently one of the two sums involved in Eq. (6). In this way, for $\{0, 1\}$ units, one has

$$Z = \sum_{\mathbf{x}} e^{\mathbf{b}^T \mathbf{x}} \prod_i (1 + e^{\mathbf{c}_i + \mathbf{W}_i \mathbf{x}}) \quad , \quad (7)$$

where index i runs over the whole set of hidden units, and \mathbf{W}_i is the i th row of \mathbf{W} . However, the evaluation of Z is still computationally prohibitive when the number of input and hidden variables is large, since it involves an exponentially large number of terms. For that reason, RBMs are computationally hard to evaluate or simulate accurately [20].

III. ANNEALED IMPORTANCE SAMPLING

Annealed Importance Sampling was developed by R. Neal in the late 90's [10], [11]. AIS allows sampling from a probability distribution that would be otherwise intractable. Assume we want to evaluate the average value of some quantity $\alpha(\mathbf{x})$ over a probability distribution $p(\mathbf{x})$. This computation can be very inefficient due to two main reasons. On one hand, the probability distribution $p(\mathbf{x})$ can be impossible to sample because the exact form of $p(\mathbf{x})$ is not known, as it happens, for instance, in many quantum physics problems [21]–[23]. On the other hand, the number of samples required to obtain an accurate estimate of the average value of $\alpha(\mathbf{x})$ may be unreasonably large. In order to deal with these problems, one usually resorts to some form of Importance Sampling, where the exploration of the space is guided by a known and suitable probability distribution $q(\mathbf{x})$ [24]. Without loss of generality, the average value of $\alpha(\mathbf{x})$ over $p(\mathbf{x})$ can be written in the form

$$\langle \alpha \rangle = \int d\mathbf{x} p(\mathbf{x}) \alpha(\mathbf{x}) \quad . \quad (8)$$

This quantity can be approximated by sampling from $p(\mathbf{x})$. However, in many situations, as mentioned above, it is not possible to sample efficiently or directly from $p(\mathbf{x})$. This

same quantity can be evaluated using an Importance Sampling distribution $q(\mathbf{x})$ as

$$\langle \alpha \rangle = \int d\mathbf{x} q(\mathbf{x}) \left(\frac{p(\mathbf{x}) \alpha(\mathbf{x})}{q(\mathbf{x})} \right) \quad . \quad (9)$$

In this case, samples are drawn from the probability distribution $q(\mathbf{x})$, and $p(\mathbf{x})\alpha(\mathbf{x})/q(\mathbf{x})$ is accumulated to estimate $\langle \alpha \rangle$. Importance Sampling is employed to reduce the variance of the estimator, or to reduce the number of samplings needed to achieve the same statistical accuracy.

In any case, Importance Sampling can only be performed when a suitable $q(\mathbf{x})$ is at hand, but that may not always be the case. The AIS method allows building a suitable $q(\mathbf{x})$ starting from a trivial probability distribution, and annealing with a set of intermediate distribution corresponding to decreasing temperatures.

As explained in [10], [11], in order to estimate $\langle \alpha \rangle$ starting from a trivial $p_0(\mathbf{x})$, one builds a chain of intermediate distributions $p_i(\mathbf{x})$ that interpolate between $p_0(\mathbf{x})$ and $p_n(\mathbf{x}) = p(\mathbf{x})$. A common scheme to define the intermediate distributions is to set

$$p_j(\mathbf{x}) = p_0(\mathbf{x})^{1-\beta_j} p_n(\mathbf{x})^{\beta_j} \quad , \quad (10)$$

with $0 = \beta_0 < \beta_1 < \cdots < \beta_n = 1$. The approach used in AIS is to turn the estimation of $\langle \alpha \rangle$ into a multidimensional integration of the form

$$\langle \alpha \rangle = \int d\mathbf{x}_1 \cdots d\mathbf{x}_n g(\mathbf{x}_1, \cdots, \mathbf{x}_n) \frac{f(\mathbf{x}_1, \cdots, \mathbf{x}_n)}{g(\mathbf{x}_1, \cdots, \mathbf{x}_n)} \alpha(\mathbf{x}_n) \quad , \quad (11)$$

where

$$f(\mathbf{x}_1, \cdots, \mathbf{x}_n) = p_n(\mathbf{x}_n) \prod_{j=1}^{n-1} \tilde{T}_j(\mathbf{x}_{j+1}, \mathbf{x}_j) \quad (12)$$

$$g(\mathbf{x}_1, \cdots, \mathbf{x}_n) = p_0(\mathbf{x}_1) \prod_{j=1}^{n-1} T_j(\mathbf{x}_j, \mathbf{x}_{j+1}) \quad (13)$$

are normalized joint probability distributions for the set of variables $\{\mathbf{x}_1, \dots, \mathbf{x}_n\}$. In these expressions $T_k(\mathbf{x}, \mathbf{y})$ represents a transition probability of moving from state \mathbf{x} to state \mathbf{y} , which asymptotically leads to the equilibrium probability $p_k(\mathbf{z})$. In the same way, $\tilde{T}_k(\mathbf{y}, \mathbf{x})$ represents the reversal of $T_k(\mathbf{x}, \mathbf{y})$. The detailed balance condition implies that the transition probabilities fulfill the relation

$$\tilde{T}_j(\mathbf{y}, \mathbf{x}) = T_j(\mathbf{x}, \mathbf{y}) \frac{p_j(\mathbf{x})}{p_j(\mathbf{y})} \quad (14)$$

in order to be able to sample the space ergodically [25]. Therefore, $\langle \alpha \rangle$ can be estimated from Eq. (11) because: a) the ratio appearing in Eq. (11), which represents the importance sampling weights, becomes the product of the ratios of the intermediate probability distributions

$$\frac{f(\mathbf{x}_1, \dots, \mathbf{x}_n)}{g(\mathbf{x}_1, \dots, \mathbf{x}_n)} = \prod_{k=1}^n \frac{p_k(\mathbf{x}_k)}{p_{k-1}(\mathbf{x}_k)} \quad , \quad (15)$$

and b) $g(\mathbf{x}_1, \dots, \mathbf{x}_n)$ is easily sampled from the trivial $p_0(\mathbf{x})$.

In practice, one uses $g(\mathbf{x}_1, \dots, \mathbf{x}_n)$ to generate N_s samples of all the intermediate distributions, such that for every set of

values $\{\mathbf{x}_1^i, \mathbf{x}_2^i, \dots, \mathbf{x}_n^i\}$ (with i spanning the range $[1, N_s]$) one gets a set of weights $\{\omega_i\}$ upon substitution in Eq. (15). In this way, $\langle \alpha \rangle$ is estimated according to

$$\langle \alpha \rangle \sim \frac{\sum_{i=1}^{N_s} \omega_i \alpha(\mathbf{x}_n^i)}{\sum_{i=1}^{N_s} \omega_i}, \quad (16)$$

with

$$\omega_i = \prod_{k=1}^n \frac{p_k(\mathbf{x}_k^i)}{p_{k-1}(\mathbf{x}_k^i)}. \quad (17)$$

This expression can be written in term of the unnormalized probabilities $\tilde{p}_k(\mathbf{x}) = Z_k p_k(\mathbf{x})$ as

$$\omega_i = \frac{Z_0}{Z_n} \prod_{k=1}^n \frac{\tilde{p}_k(\mathbf{x}_k^i)}{\tilde{p}_{k-1}(\mathbf{x}_k^i)} = \frac{Z_0}{Z_n} \tilde{\omega}_i, \quad (18)$$

which defines the set of importance weights $\{\tilde{\omega}_i\}$ obtained from the product of the ratios of the unnormalized probabilities. Notice that $\tilde{\omega}_i$ is an accessible quantity, while ω_i is not, just because one does not have access to Z_n . One important consequence of this formalism is that a simple estimator of the partition function Z_n associated to the distribution $p_n(\mathbf{x}) = p(\mathbf{x})$ is directly given by the average value

$$\frac{Z_n}{Z_0} \sim \frac{1}{N_s} \sum_i \tilde{\omega}_i. \quad (19)$$

Usually, though, the values of $\tilde{\omega}_i$ are so large that one typically has to draw samples of $\log(\tilde{\omega}_i)$ instead. In this way, one defines a set of Z_0 -normalized AIS samples $s_i = \log(\tilde{\omega}_i) + \log(Z_0)$, such that

$$\log(Z_{\text{AIS}}) = \log \langle Z_n \rangle_s = \log \left[\frac{1}{N_s} \sum_i e^{s_i} \right] \approx \log(Z_n), \quad (20)$$

which is the logarithmic mean of the exponentiated samples. Notice that this value is different from the mean of the samples s_i , although in many cases is similar. In fact, these two quantities tend to be the same when the variance of the set of samples is small compared to the mean value. In other situations, the nonlinear character of the operation in Eq. (20) makes the result be dominated by the largest samples, to the point that, in the extreme case, the largest sample exhausts the total sum.

IV. EFFICIENT USE OF AIS IN RBMS

For the special case of the RBM, the equilibrium Boltzmann distribution associated to the visible layer is given by

$$p(\mathbf{x}) = \sum_{\mathbf{h}} p(\mathbf{x}, \mathbf{h}) = \frac{1}{Z} \sum_{\mathbf{h}} e^{-E(\mathbf{x}, \mathbf{h})} \quad (21)$$

with the energy function of Eq. (2). In the spirit of AIS, the partition function associated with $p(\mathbf{x})$ can be obtained from a chain of intermediate probability distributions. An easy-to-sample distribution $p_0(\mathbf{x})$, built from a RBM model containing only visible bias terms \mathbf{B} , turns out to be a convenient starting point. In this way one generates a family of energy functions

$$-E_k(\mathbf{x}, \mathbf{h}) = (1 - \beta_k) \mathbf{B}^T \mathbf{x} + \beta_k (\mathbf{b}^T \mathbf{x} + \mathbf{c}^T \mathbf{h} + \mathbf{h}^T \mathbf{W} \mathbf{x}), \quad (22)$$

with $\beta_k = k/n$ and $k = 0, 1, \dots, n$. Notice that this prescription is not exactly the same as the one reported in Eq. (10), although this is not relevant since the AIS algorithm does not impose a specific scheme. As expected, one recovers $p(\mathbf{x})$ for $k = n$.

In this scheme, $E_0(\mathbf{x}, \mathbf{h}) = \mathbf{B}^T \mathbf{x}$, which makes $p_0(\mathbf{x})$ a probability distribution that is trivial to sample, with $Z_0 = 2^{N_h} \prod_{j=1}^{N_v} (1 + e^{B_j})$. In this sense, this procedure is similar to the one presented in [12]. According to Eq. (19) and considering Z_0 is known, one can use AIS to sample Z from the set of importance weights $\{\tilde{\omega}_i\}$. In practice, one uses Gibbs sampling to implement the transition probabilities $T_k(\mathbf{x}_k, \mathbf{x}_{k+1})$ at each k , so that \mathbf{x}_{k+1} is obtained from \mathbf{x}_k efficiently. In this way, one starts from a certain \mathbf{x}_1 sampled from $p_0(\mathbf{x})$ and get \mathbf{x}_2 from $T_1(\mathbf{x}_1, \mathbf{x}_2)$, use this new value to obtain \mathbf{x}_3 from $T_2(\mathbf{x}_2, \mathbf{x}_3)$, and so on. Notice once again that sampling \mathbf{x}_1 is trivial since $p_0(\mathbf{x})$ contains only visible bias terms \mathbf{B} .

In general, AIS depends on three parameters which define the computational cost and accuracy of the approximation. A remarkable one is the set of bias \mathbf{B} , as a suitable selection can improve the quality of the samples obtained, and the overall calculation. Another relevant parameter is the number N_β of intermediate probability distributions, which has to be fixed beforehand. Finally, the number of samples N_s has also to be set.

Getting a suitable \mathbf{B} may not be a trivial task, and in this work we elaborate on this point. In fact, the problem of getting \mathbf{B} can be mapped into the problem of determining the mean value of the visible units. This relation can be established minimizing the Kullback-Leibler (KL) divergence between $p_0(\mathbf{x})$ and the full RBM probability distribution $p_n(\mathbf{x})$

$$\nabla_{\mathbf{B}} \sum_j p_n(\mathbf{x}_j) \log \left(\frac{p_n(\mathbf{x}_j)}{p_0(\mathbf{x}_j)} \right) = 0,$$

where the sum over j extends to all the 2^{N_v} states obtained after marginalization over the hidden units. With $p_0(\mathbf{x}) = 2^{N_h} e^{-\mathbf{B} \cdot \mathbf{x}} / Z_0$, the above condition leads to

$$\begin{aligned} 0 &= - \sum_j p_n(\mathbf{x}_j) \nabla_{\mathbf{B}} \ln p_0(\mathbf{x}_j) \\ &= \sum_j p_n(\mathbf{x}_j) \mathbf{x}_j + \sum_j p_n(\mathbf{x}_j) \nabla_{\mathbf{B}} \log Z_0 \\ &= \langle \mathbf{x} \rangle_n - \left\langle \frac{1}{e^{\mathbf{B}} + 1} \right\rangle_n, \end{aligned} \quad (23)$$

where the subscript n indicates that the average values are taken over the $p_n(\mathbf{x})$ probability distribution corresponding to the target RBM. In this way, the optimal bias \mathbf{B} are given by the expression

$$B_i = \log \left(\frac{1}{\langle x_i \rangle_n} - 1 \right) \quad (24)$$

for each visible unit $i \in 1, 2, \dots, N_v$. The problem of finding the optimal \mathbf{B} is thus equivalent to obtaining the exact average values of the visible units. Since this problem is as hard as finding Z itself, one has to devise alternative strategies to approximate $\langle x_i \rangle_n$.

Two common strategies are usually employed to face this problem. The simplest one is to simply set $\mathbf{B} = 0$ and sample from the uniform probability distribution. This is a very cheap procedure that has nevertheless some drawbacks as will be shown later. Another common strategy was devised in [12], where the dataset used to train the RBM is employed to find $\langle \mathbf{x} \rangle_n$. This last scheme, which usually works well in machine learning problems, has two potential issues: on one hand, it can not be implemented when there is no training set; and on the other, it assumes that the training set represents a significant subset of the highest-probability states, something that presumably happens only at the end of the learning process, but definitely not at the first epochs. The first issue is specially relevant because the problem of finding Z is more general than its application to machine learning problems.

In this work we introduce alternative strategies to evaluate $\langle \mathbf{x} \rangle_n$ that prove to be as efficient as the previous ones, avoiding some of the commented drawbacks. In all cases, the main idea is to estimate $\langle \mathbf{x} \rangle_n$ by direct sampling of the RBM. In order to do that, two decisions have to be made, regarding the sampling scheme and the starting point \mathbf{x}_{ini} . As far as the sampling method is concerned, we use both Gibbs sampling and Metropolis sampling, the latter with an additional parameter which is the number of units to flip at each iteration. Regarding the initial state, the number of possibilities is larger. We have tried a few of them:

- a) $\mathbf{x}_{\text{ini}} = 0$.
- b) $\mathbf{x}_{\text{ini}} = 1$.
- c) \mathbf{x}_{ini} sampled from the Bernoulli distribution ($p = 0.5$).
- d) Mean field (MF) approximation for a high-probability state: in this scheme one assumes that the fluctuations of the hidden units with respect to their mean values is so small that one can neglect quadratic terms. One starts from the free energy of a given visible state and replaces \mathbf{h} by $\langle \mathbf{h} \rangle + \delta \mathbf{h}$, expanding the exponential of the $\delta \mathbf{h}$ terms to first order

$$\begin{aligned}
 \mathcal{F}(\tilde{\mathbf{x}}) &= \sum_{\tilde{\mathbf{h}}} e^{\tilde{\mathbf{x}}^T \tilde{\mathbf{W}} \tilde{\mathbf{h}}} = \sum_{\tilde{\mathbf{h}}} e^{\tilde{\mathbf{x}}^T \tilde{\mathbf{W}} (\langle \tilde{\mathbf{h}} \rangle + \delta \tilde{\mathbf{h}})} \\
 &\approx \sum_{\tilde{\mathbf{h}}} e^{\tilde{\mathbf{x}}^T \tilde{\mathbf{W}} \langle \tilde{\mathbf{h}} \rangle} \left(1 + \tilde{\mathbf{x}} \tilde{\mathbf{W}} \delta \tilde{\mathbf{h}} \right) \\
 &= 2^{N_h} e^{\tilde{\mathbf{x}}^T \tilde{\mathbf{W}} \langle \tilde{\mathbf{h}} \rangle} + \tilde{\mathbf{x}} \tilde{\mathbf{W}} e^{\tilde{\mathbf{x}}^T \tilde{\mathbf{W}} \langle \tilde{\mathbf{h}} \rangle} \sum_{\tilde{\mathbf{h}}} \left(\tilde{\mathbf{h}} - \langle \tilde{\mathbf{h}} \rangle \right) \\
 &= 2^{N_h} e^{\tilde{\mathbf{x}}^T \tilde{\mathbf{W}} \langle \tilde{\mathbf{h}} \rangle} .
 \end{aligned} \tag{25}$$

The resulting expression does not depend on the explicit values of $\tilde{\mathbf{h}}$, but only on their mean values, which are always positive when working with $\{0, 1\}$ units. In this way, $\mathcal{F}(\mathbf{x})$ is maximal when $x_i \sum_j \omega_{ij}$ is maximal $\forall i$. A necessary condition for this to happen is that x_i must have the same sign as $\sum_j \omega_{ij}$. Since x_i can not be negative, we simply set x_i to 1 if $\sum_j \omega_{ij} > 0$, and 0 otherwise.

- e) Pseudoinverse (PS) approximation for a high probability state: one can also look for a state of the complete (visible and hidden) space that has a large probability as the starting point of the sampling process. Things are much simpler than in d) because in this case one works directly

with the energy rather than the free energy. Setting to zero the gradients with respect to \mathbf{x} and \mathbf{h} of the energy in Eq. (2), one finds

$$\mathbf{x}_p = -(\mathbf{W}^+)^T \mathbf{c} , \quad \mathbf{h}_p = -\mathbf{W}^+ \mathbf{b} , \tag{26}$$

where \mathbf{W}^+ is the pseudoinverse of the \mathbf{W} matrix. Notice that these equations are decoupled, and that therefore one can start from either of them in a Gibbs sampling scheme. In this work we build \mathbf{x}_{ini} from \mathbf{x}_p , by rounding it to the $\{0, 1\}$ range.

In this way, the total computational cost associated to the evaluation of Z is divided in two parts, one corresponding to building \mathbf{B} , and another, proportional to $N_\beta \cdot N_s$, corresponding to the AIS algorithm. The approximation obtained improves when both N_β and N_s tend to infinity [11]. Starting the AIS algorithm from the uniform probability distribution may require extremely high values of N_β and N_s to obtain a reasonably good approximation of Z . Typical values of N_β and N_s commonly employed in previous works range from a few hundreds to several thousands, but at least one of them is always large [12], [15]. However, to the best of our knowledge, no systematic analysis on the convergence properties of the AIS algorithm applied to RBMs has been carried out so far, other than the discussion in Ref. [18].

In this work we argue that, by getting a good starting probability distribution $p_0(\mathbf{x})$ from a suitable bias \mathbf{B} , one can obtain the same accuracy with much lower values of N_β and N_s . As a consequence, the overall computational cost, including the cost associated to building the \mathbf{B} 's, turns out to be much lower. In summary, we study the compound problem of finding a good $p_0(\mathbf{x})$ and evaluating AIS, to find the best possible approximation of Z with as low computational cost as possible. The $p_0(\mathbf{x})$ probability distributions explored are always trivially sampled as they only contain visible bias terms, which are obtained using both Metropolis and Gibbs sampling methods as explained above.

We explore both artificial and large-sized realistic problems. For the artificial tests, we build systems where the exact value of the partition function can be computed and compared with the AIS results, thus being a benchmark for the latter. We analyze the convergence of the AIS estimate for fixed and small N_β and N_s starting from different $p_0(\mathbf{x})$ distributions and sampling methods, and compare to the exact result. From this analysis we extract a set of strategies and parameters that we use to obtain the estimation of Z in realistic problems. These results are compared with what we take as the ground truth, which is an AIS estimate of Z using $N_\beta = 2^{20}$ and $N_s = 1024$, starting from the corresponding training set and using the Salakhutdinov procedure outlined in [12].

A final relevant remark is to realize that the value of Z is invariant under the exchange of the visible and hidden units, provided $\tilde{\mathbf{W}}$ is transposed. This is not trivial from the point of view of the AIS algorithm since in AIS one evaluates the probabilities of the visible states, which are different in each case. As a consequence, AIS does not necessarily gives the same predictions. This can be of particular relevance when the system is highly unbalanced, as usually happens in machine learning problems, where the number of hidden units

is typically different from the number of visible units. For that reason we explore all the previous parameters and strategies both for the original and the transposed system, in the latter case including also the analysis for $\mathbf{B} = 0$, corresponding to the uniform probability distribution. Remarkably, though, the computational cost involved in AIS is the same independently of whether $\tilde{\mathbf{W}}$ is transposed or not when Gibbs sampling is employed in the intermediate chains of the algorithm.

As a side note, the reader may realize that in both steps (building \mathbf{B} and performing AIS) there is at least one dimension that can be easily parallelized. At this level, using NVIDIA[®] CUDA[®] hardware is a perfect fit for the task.

V. DESCRIPTION OF THE EXPERIMENTAL PROBLEMS ANALYZED

In order to perform a systematic study of the convergence properties of the AIS algorithm, we test its performance in several problems where one can analytically compute the exact value of the partition function. We separate the sets of weights in two categories, one corresponding to purely artificial sets, and the other to simplified realistic problems where a dimension is largely reduced.

Regarding the purely artificial systems, we explore the following cases:

1) Gaussian Weights with Gaussian Moments (GWGM)

The first artificial model employed is characterized by a weights matrix of Gaussian random numbers with $N_v = 20$ and two values of N_h , namely 60 and 180. The mean value and the standard deviation of each weights matrix are also sampled from a Gaussian distribution, as explained in the Sec. VI. Due to the reduced value of N_v , the exact calculation of Z can be performed by brute force.

2) Block Matrix Systems (BMS)

In this model the weights matrix \mathbf{W} is organized by blocks located at its diagonal. All blocks can be different, but they are of a reduced size that allows for an independent, exact evaluation of its corresponding partition function. In this way, the weights matrix takes the form

$$\mathbf{W} = \begin{pmatrix} \mathbf{W}_1 & 0 & \cdots & 0 \\ 0 & \mathbf{W}_2 & \cdots & 0 \\ \vdots & \vdots & \ddots & \vdots \\ 0 & 0 & \cdots & \mathbf{W}_{N_B} \end{pmatrix}. \quad (27)$$

If \mathbf{W} is formed by M_B blocks, the partition function of the overall system is simply

$$Z = \prod_{j=1}^{M_B} Z_j,$$

with Z_j is the partition function of each isolated block.

In this work we take each \mathbf{W}_k to be of the GWGM form.

In much the same way, the simplified realistic problems analyzed are:

3) A set of weights obtained after training a RBM with the MNIST dataset¹, with $N_h = 20$ hidden units (MNIST-20h). We monitor and store the weights at each epoch

along the learning process, and make a suitable final selection that characterizes the evolution of the weights matrix at all stages during the learning process, as described in the Sec. VI. In this way, we have snapshots of the system taken at the beginning of the learning, where the training set typically does not contain the highest probability states, and at the end, where they are supposed to carry most of the probability density mass of the system.

4) A set of weights obtained after training a RBM with the Web-w6a dataset, with $N_h = 20$ hidden units (Web-w6a-20h) in the same conditions as the MNIST-20h case. This dataset contains data from web pages with $N_v = 300$ sparse binary keyword attributes taken from [26]. We use this problem to train a RBM containing 49749 examples in the training set obtained joining all the available original examples.

Finally, we test the performance of AIS with the studied strategies on realistically large-sized problems. In particular, we analyze the MNIST and Web-w6a systems, trained with a much larger number of hidden units, $N_h = 500$ (MNIST-500h and Web-w6a-500h).

VI. EXPERIMENTAL RESULTS

A. Results for Exactly Solvable Models with $\mathbf{B} = 0$

In the following we report our results regarding the AIS estimation of the partition function for the different systems described in the previous section, where the exact Z can be numerically computed. In all cases, the dimensions of the systems have been chosen such that one dimension is large and comparable to what one finds in real-world problems. One of the major goals of this work is to obtain good approximations of Z with small values of the AIS parameters. Unless otherwise stated, the number of AIS chains and AIS samples have been set to $N_\beta = N_s = 1024$, as an overall balance between computational cost and statistical accuracy. These values are small compared to what one usually finds in the literature [12], [15]. In any case, all values are taken to be a power of 2, as we have checked that convergence towards the exact value seems to be logarithmic.

We start by analyzing the $\mathbf{B} = 0$ case, so that $p_0(\mathbf{x})$ is the uniform probability distribution. This is the simplest scheme as there is no computation of a starting bias \mathbf{B} . In the GWGM and BMS cases, all weights have been randomly chosen, following a Gaussian distribution. The mean and standard deviation of each Gaussian has also been chosen to be Gaussian, with μ_μ and σ_μ the mean and standard deviation of the mean values, and μ_σ and σ_σ the mean and standard deviation of the standard deviations. In order to mimic what one finds in realistic learning problems, the mean and standard deviation of the bias terms can be different from the ones corresponding to the \mathbf{W} weights. In this work we introduce a factor λ that scales the μ and σ of \mathbf{b} and \mathbf{c} with respect to those of \mathbf{W} ,

$$\mu_{\text{bias}} = \lambda \mu_{\mathbf{W}}, \quad \sigma_{\text{bias}} = \lambda \sigma_{\mathbf{W}}.$$

In the MNIST-20h and Web-w6a-20h cases the weights are the result of learning the corresponding problems using CD₁, at different epochs (10, 50, 100, 200, 300, 400, 500).

¹<http://yann.lecun.com/exdb/mnist>

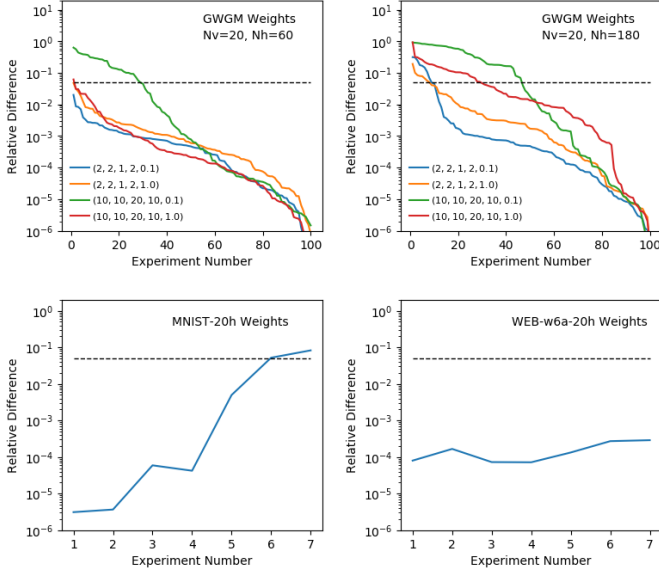


Fig. 1. Relative differences between the exact $\log(Z)$ and the AIS estimated $\log(Z)$ starting from the uniform probability distribution ($\mathbf{B} = 0$). All calculations correspond to $N_s = 1024$ AIS samples and $N_\beta = 1024$ intermediate probability distributions. The horizontal dashed line indicates a relative difference of 5%, see the text for further details.

We show in Fig. 1 a selection of the results obtained for some of the exactly solvable models analyzed. For GWGM, the specific values of $(\mu_\mu, \sigma_\mu, \mu_\sigma, \sigma_\sigma, \lambda)$ are given in the plot. In all cases, the vertical axis indicates the relative differences $\xi = |(\log(Z_{\text{Ex}}) - \log(Z_{\text{AIS}})) / \log(Z_{\text{Ex}})|$, with $\log(Z_{\text{Ex}})$ and $\log(Z_{\text{AIS}})$ the exact and AIS-estimated results, respectively. For the GWGM weights, the horizontal axis corresponds to the experiment number, sorted according to the value of ξ . The MNIST-20h and Web-w6a-20h cases are sorted according to the epoch number. In the latter cases, the estimated likelihood stabilizes in the final epochs. In all plots, a horizontal dashed line indicating a relative difference of 5% has been included. We take this value as a (subjective) threshold for a suitable approximation of $\log(Z)$.

As it can be seen from the figure, two different behaviours arise. In many cases there is a large region where the AIS algorithm starting from the uniform probability distribution performs very well, leading to very small relative differences with respect to the exact values. This is particularly notorious in the Web-w6a-20h case. In the MNIST-20h, differences arise at the end of the learning, but they are relatively small. On the contrary, the GWGM problems show a behaviour that depends on the size of the system and the parameters defining the Gaussian weights, as can be seen in the upper panels. Notice, though, that the most divergent curves correspond to the larger systems, a tendency that we have verified also in the BMS case. One may think that the weight values in these experiments are large (in absolute value) compared to what one usually finds in RBM learning problems. Still, one should keep in mind that in realistic learning problems, the tendency of the absolute value of the weights is to

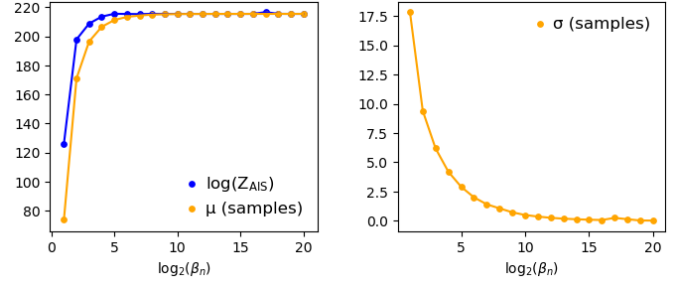


Fig. 2. left panel: AIS estimation of $\log(Z)$, starting from the uniform probability distribution, for the MNIST-20h weights at epoch 500 (blue points), and mean of the samples (orange points). Right panel: standard deviation of the same set of samples. Results have been obtained with $N_s = 1024$ samples and the values of N_β span the range $(2^1, 2^{20})$.

increase along learning. As an example, the Root Mean Square value of the MNIST-20h weights at the epochs considered is $(0.22, 0.38, 0.48, 0.59, 0.66, 0.71, 0.76)$, while for the Web-w6a these values are smaller. This fact has to be taken into account if one seeks to perform a calculation of Z along learning, as the problem hardens as learning progresses. Parenthetically, we have verified that, at least for the purely artificial problems, the agreement between $\log(Z_{\text{Ex}})$ and $\log(Z_{\text{AIS}})$ improves when the parameters of the Gaussian distribution used to build the weights are very small. The BMS systems formed by GWGM blocks show a remarkably similar behaviour to the upper panels in the figure. Packing GWGM weights with a similar ξ in a BMS structure leads to approximately the same value of ξ . In this way, building blocks out of smaller arrangements does not seem to alter the intrinsic difficulty of the problem.

Another potential issue of starting from the uniform probability distribution is that the estimation obtained seems to converge fast to a possibly wrong value when increasing N_β . Theoretical arguments indicate that, in the long run, the estimation must converge to the exact value, but this convergence can be extremely slow. In this way, one can perform a calculation and get the wrong impression that the result obtained is close to the exact one. This is shown in the left panel of Fig. 2, where $\log(Z_{\text{AIS}})$ and the mean of the AIS samples for the MNIST-20h problem at epoch 500 are depicted as a function of the number of intermediate chains used, for fixed $N_s = 1024$ samples. One could infer from the plot that AIS is yielding a good and stable estimation, which is $\log(Z_{\text{AIS}}) \approx 215.17$, while the exact value is $\log(Z_{\text{Ex}}) = 234.85$. To make things worse, the standard deviation of the samples decreases with increasing number of AIS chains and approaches zero, as shown in the right panel of the figure. Notice that not even with $N_\beta = 2^{20}$ the AIS prediction changes appreciably to approach the exact value. This reinforces the false impression that $\log(Z)$ is accurately estimated. Although not reported here, we have seen that this is a common behaviour found in other problems.

In summary, the analyzed set of exactly solvable models indicates that, while the uniform probability distribution may

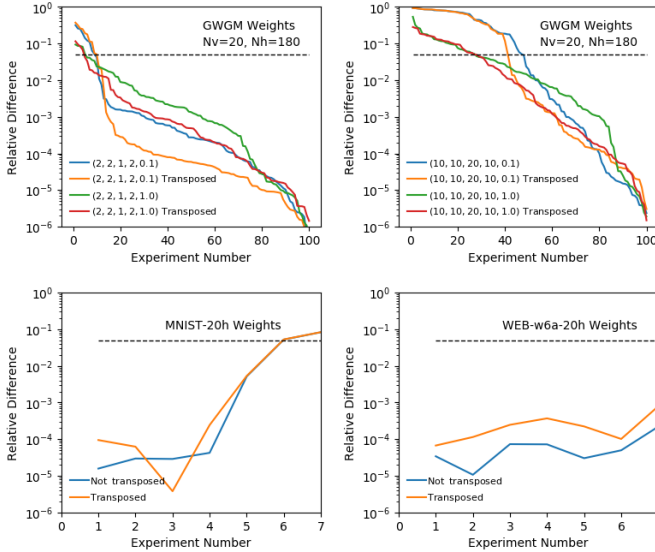


Fig. 3. Relative differences ξ between $\log(Z_{\text{Ex}})$ and $\log(Z_{\text{AIS}})$ starting from the uniform probability distribution ($\mathbf{B} = 0$) for transposed and non-transposed systems. All calculations correspond to $N_s = 1024$ AIS samples and $N_\beta = 1024$ intermediate probability distributions. The horizontal dashed line indicates a relative difference of 5%.

seem to be a good starting point for AIS, this is not the case in general. In fact, using a finite but large number of AIS chains does not guarantee that one approaches the exact result. Even worse, one can get the false impression that already a simple calculation with a small number of chains leads to a stable result close to the exact one (as shown in Fig. 2), while this may definitely not be the case. We have checked that this situation is not solved by increasing the number of samples, either. Depending on the desired accuracy, these facts call for a better initialization of the AIS algorithm. We elaborate on this point in the next sections.

B. Analysis of the Transposed System for $\mathbf{B} = 0$ in Exactly Solvable Models

We start by analyzing the simplest alternative, which is to transpose the system while keeping $\mathbf{B} = 0$. Transposing the system implies exchanging the visible and hidden layers, and to replace $\tilde{\mathbf{W}}$ with its transpose $\tilde{\mathbf{W}}^T$. For the sake of comparison, we show in Fig. 3 the performance of AIS when the original and the transposed system is sampled from the uniform probability distribution, for the most difficult artificial cases of Fig. 1 in the upper panels, and for the MNIST-20h and the Web-w6a-20h in the lower panels. As in Fig. 1, a horizontal dashed line indicating the value $\xi = 0.05$ is also displayed. Results show very little improvement since the most marked differences appear for quite low values of ξ , whereas for larger ξ 's the differences are less significant. Note that in the purely artificial systems, in contrast to the MNIST-20h and Web-w6a-20h cases, the number of visible units in the transposed system is much larger than in the original one. Still, none of the plots indicate that transposing leads to a statistically meaningful better solution when starting from the

uniform probability distribution. As we will show later, this is not the case when using other strategies and parameters. In any case, transposing is a very simple operation that does not substantially change the AIS complexity, does not seem to worsen the estimation, and that can always be considered as a cheap alternative to the standard procedure.

C. Results for Exactly Solvable Models with $\mathbf{B} \neq 0$

In this section we explore and discuss the different AIS predictions one obtains starting from a non-uniform probability distribution given by $\mathbf{B} \neq 0$. The bias \mathbf{B} are obtained using the strategies (Gibbs Sampling and Metropolis) and the initializations outlined in section IV. Each strategy has its own parameters, and we vary them over a wide range of values in order to determine their relevance on \mathbf{B} and on the resulting $\log(Z_{\text{AIS}})$. Two common parameters for both strategies are the number of samples and the number of steps between samples. In the Metropolis case there is an additional parameter, which is the number of bits to flip in each proposal. Eventually, these values can depend on the size of the problem, and we report the ones we have used in table I. In each case we generate a set of samples that are used to compute the mean values $\langle x_i \rangle_n$ used in Eq. (24). In practice, though, Eq. (24) can not be directly used as $\langle x_i \rangle_n = 0$ and $\langle x_i \rangle_n = 1$ give divergent bias. In this way, one has to regularize that expression, introducing a cutoff value to avoid this problem. In this work we use a cutoff ϵ to linearly rescale the $[0, 1]$ interval into the $[\epsilon, 1 - \epsilon]$ one, with ϵ ranging from 0.01 to 0.20, as shown in Table I.

Armed with all these combinations, we perform a search of the best-overall sets that improve as much as possible over the $\mathbf{B} = 0$ case. The aim of this search is to find a combination of values that works well in most cases, and that can be used as a suitable starting point for any AIS calculation. Of course, one can not guarantee that these values will be the best ones for any specific problem, but we expect them to work well in similar cases.

In order to find the best possible combinations of strategies, initializations and parameters, we perform an exhaustive analysis of all possible 325 combinations in several problems, including the GWGM, BMS and the MNIST-20h datasets. For the GWGM case we have selected three sets of weights extracted from the most difficult curve of Fig. 1, corresponding to $N_v = 20$, $N_h = 180$ and $(\mu_\mu, \sigma_\mu, \mu_\sigma, \sigma_\sigma, \lambda) = (-10, 10, 20, 10, 0.1)$. These sets yield a value of $\xi = 0.92, 0.55, 0.06$ in the curve. The BMS case is built from three GWGM weights with $\xi = 0.923, 0.922$ and 0.904 . For the MNIST-20h case, we have selected the set of weights at 500 epochs, where the $\mathbf{B} = 0$ estimations are worse. Figure 4 shows the AIS results, obtained from all possible strategies and parameters of table I and initializations of section IV, for the GWGM (panels (a), (b) and (c)), BMS (panel (d)) and MNIST-20h (panel (e)) sets of weights. The black dashed line in the plots indicates the value of $\log(Z_{\text{Ex}})$, while the green dotted one corresponds to $\xi = 0.05$ as in Fig. 1.

As it can be seen, for the GWGM problem all combinations work in the easy case of panel (a), while the accuracy in

Strategy	#Samples	#Steps	Number of Bit Changes	ϵ
Gibbs sampling	1024	1, 10, 100	-	0.01, 0.05, 0.10, 0.20
Metropolis	1024	10, 100	5%, 10%, 15%, 25%, 50%, 100% (GWGM and BMS) 1, 10, 40, 80 (MNIST-20h and Web-w6a-20h)	0.01, 0.05, 0.10, 0.20

TABLE I

DESCRIPTION OF THE PARAMETERS USED IN THE EXPERIMENTS FOR THE TWO STRATEGIES EMPLOYED.

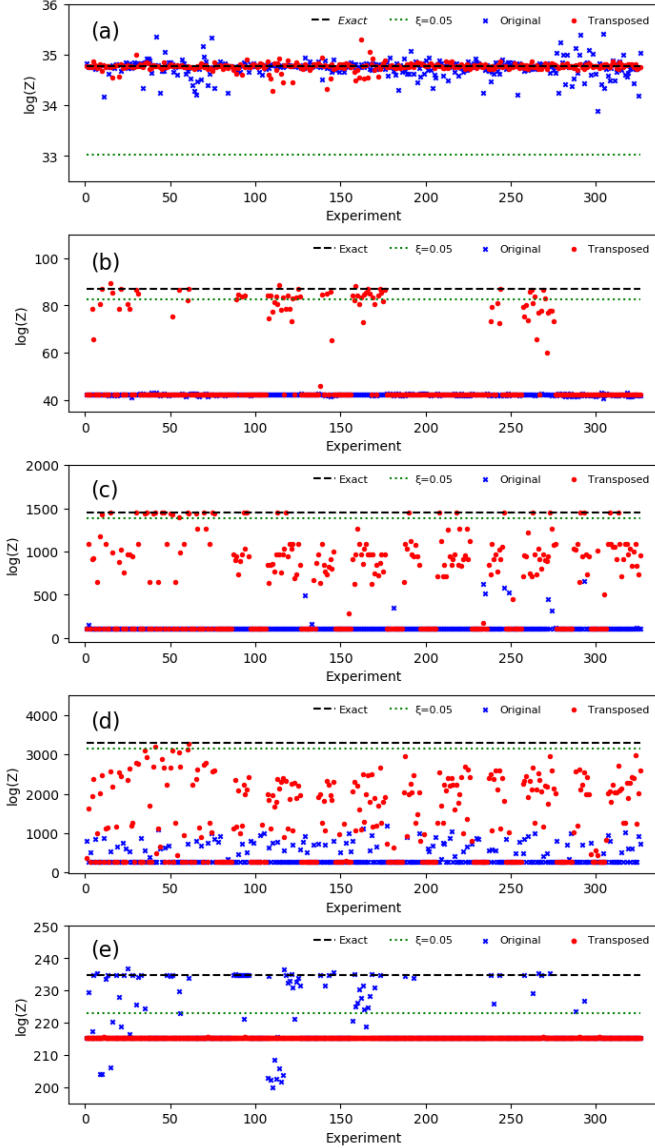


Fig. 4. Results of all possible strategies, initializations and parameters for the selected sets of weights in figure 1 (see text for details). Black dashed line: exact value of $\log(Z_{\text{Ex}})$; green dotted line: value of $\log(Z_{\text{AIS}})$ that leads to a relative difference of 5%; blue crosses: original weights; red circles: transposed weights.

the intermediate and hardest ones (panels (b) and (c)) is dramatically reduced. In this sense, there is a strong correlation between difficulty and the number of working combinations. Remarkably, transposing the weights leads to overall better estimations. In fact, in almost all cases the estimation for the transposed system is closer to $\log(Z_{\text{Ex}})$ than the original one,

a behaviour that is not reproduced when starting from $\mathbf{B} = 0$. In this sense and for these problems, transposing seems to be a proper choice when combined with the proposed strategies. This may be related to the fact that, in the cases analyzed, transposing makes the number of visible units to be larger than the number of hidden units, providing more degrees of freedom to both \mathbf{B} and the AIS samples. The same conclusions apply to the BMS plot of panel (d), as the transposed system is remarkably better predicted than the original one. The MNIST-20h points in panel (e) show that this problem is not easy, as with the GWGM cases in panels (b) and (c). In this case, transposing the weights leads to the dramatically stable and bad prediction of around 215.17 of Figs. 1 and 2. Again, this can be traced back to the fact that the original system already has $N_v = 784 \gg N_h = 20$ units.

Despite the fact that one can find good strategies for specific sets of weights, it is very unlikely to get overall winning strategies that work well in all cases. In fact, the physics described by arbitrary weights can be very different, ranging from paramagnetic to ferromagnetic states or spin glasses. The selection of good strategies, therefore, is similar to the model selection procedure in a typical Machine Learning scenario. In this way, an exhaustive search should be performed if one seeks to obtain the best possible estimation of $\log(Z)$. We show in Fig. 5 a selection of good working strategies for the $N_v = 20$, $N_h = 180$, $(\mu_\mu, \sigma_\mu, \mu_\sigma, \sigma_\sigma, \lambda) = (-10, 10, 20, 10, 0.1)$ GWGM weights, together with the MNIST-20h and the Web-w6a-20h ones. In each case we have chosen the two Gibbs sampling and two Metropolis strategies that work best for that particular problem, with the corresponding parameters reported in table II. As in the previous plots, we also include the prediction for the $\mathbf{B} = 0$ system of Fig. 3, and indicate with a black dashed line a relative difference limit of 5% with respect to the exact value of $\log(Z)$. Notice that the GWGM weights have been transposed, while the original configurations have been kept for the MNIST-20h and Web-w6a-20h sets. On the one hand, one readily notices that the selected strategies work very well in Web-w6a-20h problem, as does the $\mathbf{B} = 0$ estimation. On the other hand, the MNIST-20h is well reproduced by the selected strategies, even at the final epochs where the $\mathbf{B} = 0$ estimations fails. The most complex scenario is found on the GWGM case, where at least a 40% of the predictions made by the $\mathbf{B} = 0$ AIS calculations lay above the accuracy threshold of 5%. In this case one observes a neat improvement of the selected strategies along two different directions: first, the number of estimations above the 5% limit is reduced, and second, the relative differences ξ are also lower

Problem	Strategy+Initialization	#Samples	#Steps	Number of Bit Changes	ϵ
GWGM	Gibbs MF	1024	1	-	0.10
	Gibbs ZERO	1024	1	-	0.10
	Metropolis MF1	1024	10	15%	0.05
	Metropolis MF2	1024	10	100%	0.10
MNIST-20h	Gibbs MF	1024	100	-	0.05
	Gibbs PS	1024	100	-	0.05
	Metropolis MF	1024	100	1	0.10
	Metropolis PS	1024	100	1	0.10
Web-w6a-20h	Gibbs MF	1024	100	-	0.05
	Gibbs PS	1024	100	-	0.05
	Metropolis MF	1024	100	1	0.10
	Metropolis PS	1024	100	1	0.05

TABLE II

DESCRIPTION OF THE PARAMETERS USED IN THE BEST STRATEGIES FOUND FOR VERY PROBLEM.

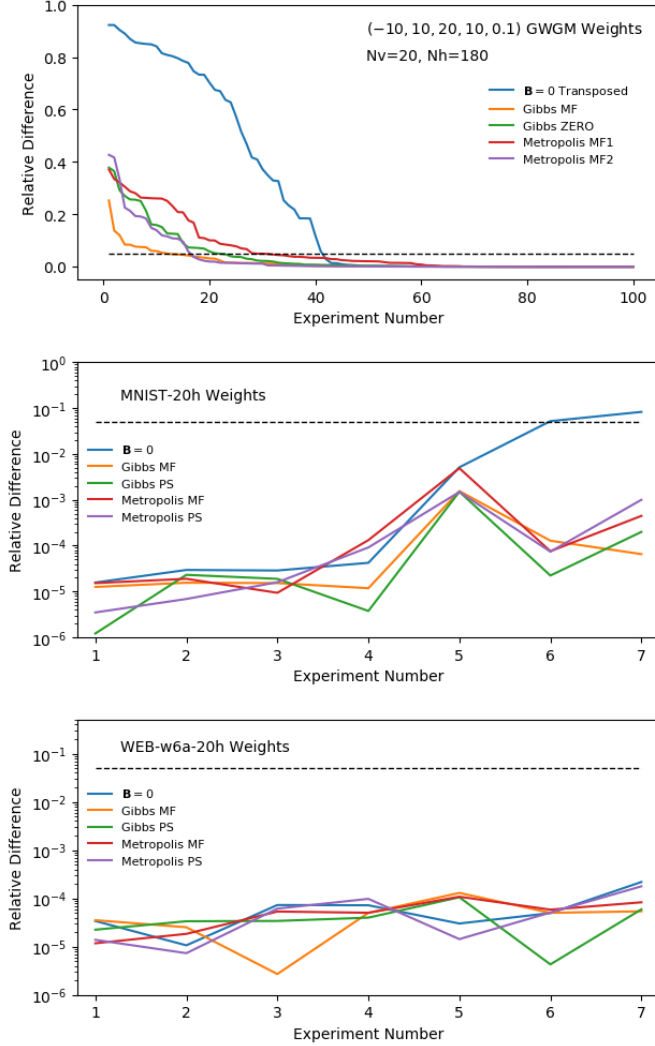


Fig. 5. Results of the selected good working strategies for GWGM (upper panel), MNIST-20h (middle panel) and Web-w6a-20h (lower panel) weights, see text for details. The black dashed line indicates a relative difference $\xi = 5\%$ with respect to $\log(Z_{\text{Ex}})$.

than in the $\mathbf{B} = 0$ case.

In summary, for all the problems at hand, one can always find a combination of strategies, initializations and parameters that give a better AIS prediction that any estimation obtained

starting from $\mathbf{B} = 0$. In this sense, one may wonder whether it is possible to find a set of strategies that generically perform better than the $\mathbf{B} = 0$ ones in most cases. As shown above, the best strategies are problem-dependent, a situation that is difficult to overcome and common to other Machine Learning situations.

From our experiments we have observed that Metropolis sampling can perform better than Gibbs sampling, at the cost of choosing the value of an additional parameter, namely the number of units to flip at each step. Furthermore, the cutoff ϵ also plays a significant role, while it is meant to avoid singular values of \mathbf{B} but not to introduce or modify the underlying physics of the problem. Regarding the initializations, the most successful ones correspond to the MF or PS choices, which is an interesting feature as they depend explicitly on the matrix of weights. Finally, transposing seems to be the best choice when the number of hidden units in the original system is larger than the number of visible ones. Based on these observations and for the sake of completeness, we have selected a couple of strategies, Gibbs_{mf} and Gibbs_{ps} , that perform better than the uniform probability distribution in general, and that could be taken as the starting point in generic AIS calculations. Both strategies are based on Gibbs sampling, and use $\epsilon = 0.05$ to avoid excessive modification of the mean values $\langle x_i \rangle_n$ of Eq. (24). Finally and as mentioned above, one uses the MF initialization and the other uses PS. In both, the number of intermediate steps between samples have been set to 100, and the number of samples to average have been set to 1024. In much the same way, the number of AIS chains and AIS samples is always set to 1024 as the main goal of this work is to obtain good approximations of $\log(Z)$ with low computational cost.

Results from these two strategies are compared in Fig. 6 with the prediction of the $\mathbf{B} = 0$ system for the GWGM weights with $N_v = 20$, $N_h = 180$ and $(\mu_\mu, \sigma_\mu, \mu_\sigma, \sigma_\sigma, \lambda) = (-10, 10, 20, 10, 0.1)$, the MNIST-20h and the Web-w6a-20h cases (upper, middle and lower panels, respectively). As can be seen from the figure, both strategies perform well in the MNIST-20h and Web-w6a-20h cases, and better than the uniform probability distribution. Both strategies improve also over the $\mathbf{B} = 0$ estimation for the GWGM case, but

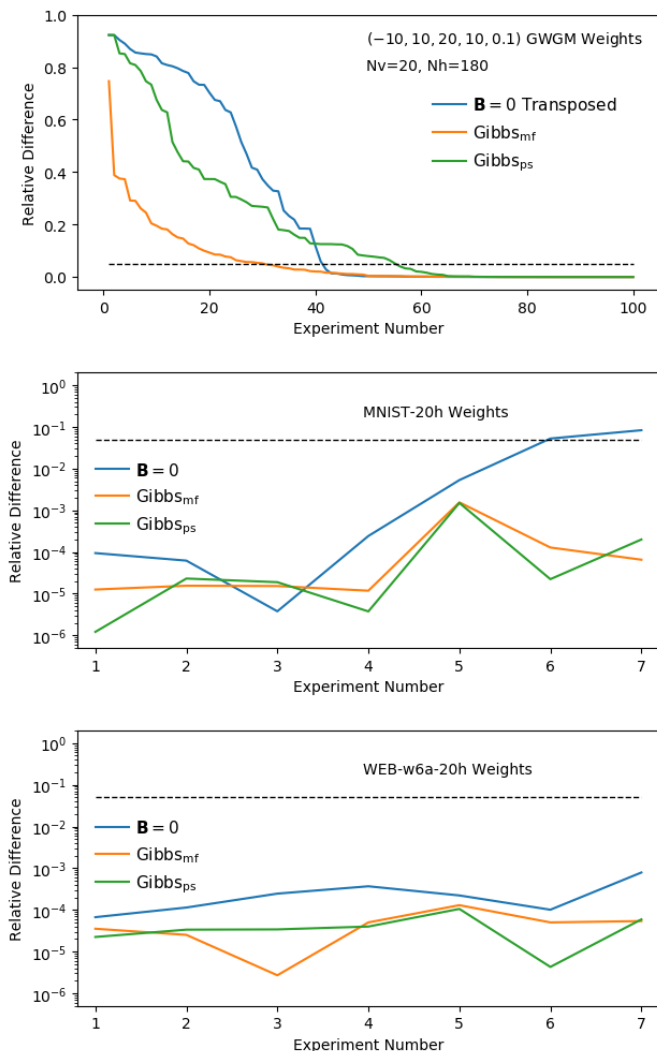


Fig. 6. Results of the two selected strategies Gibbs_{mf} and Gibbs_{ps} for GWGM (upper panel), MNIST-20h (middle panel) and Web-w6a-20h (lower panel) weights, as explained in the text. The black dashed line indicates a relative difference $\xi = 5\%$ with respect to $\log(Z_{\text{Ex}})$.

in different ways. The MF curve improves along the two directions previously mentioned, as there are few sets of weights with a relative difference error $\xi < 5\%$, while the rest have a ξ value that is clearly lower than the one of the $\mathbf{B} = 0$ curve. On the contrary, the PS curve presents more cases with $\xi > 5\%$, although most of these have a lower value than the $\mathbf{B} = 0$ prediction. In any case, a relative difference error close to 5% is still affordable in most situations, so a small increment in the number of cases around that value is less dramatic than accepting larger errors. In this way, we understand that the PS curve is, overall, better than the $\mathbf{B} = 0$ one. According to these results we conclude that, at least for the problems analyzed in this work, the MF strategy is the preferred one. We believe that it can be used as a suitable starting point for AIS calculations in other problems.

Armed with the selected strategies, we move to the more realistic Machine Learning, non-artificial MNIST-500h and

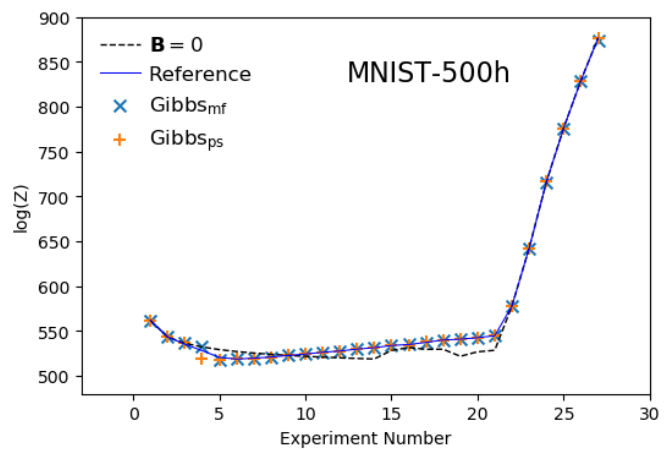


Fig. 7. Results of the two selected strategies Gibbs_{mf} and Gibbs_{ps} for the MNIST-500h weights at different epochs along learning.

Web-w6a-500h problems. For these systems there is no exact calculation of $\log(Z)$ and one has to rely to the values obtained from state-of-the-art techniques found in the literature. For that matter we take as reference the value obtained from the procedure of Ref. [12], which uses the dataset employed to train the RBM as the starting point to compute the mean values required in the evaluation of \mathbf{B} of Eq. (24). With this \mathbf{B} , we run AIS with $N_s = 1024$ and $N_\beta = 2^{20}$ to obtain the reference value.

We show in Fig. 7 the reference values, the $\mathbf{B} = 0$ estimation and the prediction of our two selected strategies for the MNIST-500h problem and a few selected epochs along the learning process. The first twenty points correspond to the first twenty epochs where $\log(Z)$ rapidly evolves, while the last points correspond to epoch numbers 40, 100, 200, 300, 400 and 500. As it can be seen, all curves merge at the highest epochs, while the $\mathbf{B} = 0$ prediction departs from the reference curve at the early and intermediate epochs. On the contrary, the selected strategies are hardly distinguishable from the reference line along the whole curve. The same comparison for the Web-w6a-500h shows excellent agreement between all curves, including the $\mathbf{B} = 0$ prediction.

VII. SUMMARY AND CONCLUSIONS

In summary, in this work we analyze the performance of the AIS algorithm in the evaluation of the partition function Z of a Restricted Boltzmann Machine with a reduced number of samples and intermediate chains. We evaluate $\log(Z)$ for a number of exactly solvable models, including Gaussian weights, Block Matrix Systems and realistic problems (MNIST and Web-w6a) with a reduced number of hidden units. In particular we show that a suitable starting probability distribution $p_0(\mathbf{x})$ can lead to a big improvement of the AIS estimation of $\log(Z)$ for fixed number of samples and intermediate chains. We build $p_0(\mathbf{x})$ from a RBM with bias terms only, and show that these values are directly related to the averages of the visible states. We note that the reference distribution of Ref. [12] is directly related to our procedure when the training set is employed to

evaluate the required averages. Remarkably, our methodology can be used when no training set is available.

For that matter, we propose sample the RBM, where only the weights and bias are required. Two standard sampling techniques are tested, Metropolis and Gibbs sampling, with different initialization schemes and cutoff parameters. We show that suitable combinations of parameters can be found such that the AIS estimation of $\log(Z)$ improves over the one obtained from the uniform probability distribution. However, while the best combinations appear to be problem dependent, we find that there are a few of them that work well in all the problems tested. We select two strategies based on Gibbs sampling that represent a trade-off between simplicity, reduced computational cost, and accuracy. We finally test them on the MNIST and Web-w6a with 500 hidden units to show that the estimations obtained are in excellent agreement with the ones from the procedure in Ref. [12]. These predictions are different from the results one gets starting from the uniform probability distribution. We expect that the strategies proposed can be used as the starting point in further studies of $\log(Z)$ in RBMs with the AIS algorithm.

Our analysis shows that the accuracy of the AIS prediction can vary considerably depending on the set of weights employed. In much the same way, the distribution of the samples obtained in AIS shows different structures for different set of weights. In fact, we have seen that the system may undergo one or more thermal phase transitions along the AIS simulation, as the β_k parameters can be understood as the inverse of the system's temperature at each step. For this reason and as a future line of work, we believe that it could be interesting to adapt the initialization algorithm to the different physical scenarios such that one starts from the proper physical phase described by the set of weights.

ACKNOWLEDGMENTS

FM: This work has been supported by MINECO grant FIS2017-84114-C2-1-P from DGI (Spain). ER: This work was partially supported by MINECO project PID2019-104551RB-I00 (Spain). Part of the hardware used for this research was donated by the NVIDIA[®] Corporation.

REFERENCES

- [1] P. Smolensky, "Information Processing in Dynamical Systems: Foundations of Harmony Theory," in *Parallel Distributed Processing: Explorations in the Microstructure of Cognition (vol. 1)*, D. E. Rumelhart and J. L. McClelland, Eds. MIT Press, 1986, pp. 194–281.
- [2] G. E. Hinton, S. Osindero, and Y. Teh, "A Fast Learning Algorithm for Deep Belief Nets," *Neural Computation*, vol. 18, no. 7, pp. 1527–1554, 2006.
- [3] G. E. Hinton and R. R. Salakhutdinov, "Reducing the Dimensionality of Data with Neural Networks," *Science*, vol. 313, no. 5786, pp. 504–507, 2006.
- [4] G. E. Hinton, "Training Products of Experts by Minimizing Contrastive Divergence," *Neural Computation*, vol. 14, pp. 1771–1800, 2002.
- [5] D. J. Earl and M. W. Deem, "Parallel tempering: Theory, applications, and new perspectives," *Physical Chemistry Chemical Physics*, vol. 7, pp. 3910–3916, 2005.
- [6] G. Desjardins, A. Courville, Y. Bengio, P. Vincent, and O. Delalleau, "Parallel Tempering for Training of Restricted Boltzmann Machines," in *International Conference on Artificial Intelligence and Statistics (AISTATS)*, 2010, pp. 145–152.

- [7] G. Desjardins, A. Courville, and Y. Bengio, "on tracking the partition function," in *Advances in Neural Information Processing Systems*, 2011, p. 25012509.
- [8] H. Huang and T. Toyozumi, "Advanced mean-field theory of the restricted boltzmann machine," *Phys. Rev. E*, vol. 91, p. 050101, 2015.
- [9] D. P. Landau, S.-H. Tsai, and M. Exler, "A new approach to monte carlo simulations in statistical physics: Wang-landau sampling," *American Journal of Physics*, vol. 72, pp. 1294–1302, 2004.
- [10] R. M. Neal, "Annealed Importance Sampling," 1998, technical Report 9805, Dept. Statistics, University of Toronto.
- [11] —, "Annealed Importance Sampling," *Statistics and Computing*, vol. 11, pp. 125–139, 2001.
- [12] R. Salakhutdinov and I. Murray, "On the Quantitative Analysis of Deep Belief Networks," in *International Conference on Machine Learning*, 2008, pp. 872–879.
- [13] R. Salakhutdinov and H. Larochelle, "Efficient Learning of Deep Boltzmann Machines," in *International Conference on Artificial Intelligence and Statistics (AISTATS)*, 2010, pp. 693–700.
- [14] R. R. Salakhutdinov and G. E. Hinton, "An Efficient Learning Procedure for Deep Boltzmann Machines," *Neural Computation*, vol. 24, no. 8, pp. 1967–2006, 2012.
- [15] M.-A. Côté and H. Larochelle, "An Infinite Restricted Boltzmann Machine," *Neural computation*, vol. 28, pp. 1265–1288, 2016.
- [16] C. Xie, J. Lv, and X. Li, "Finding a Good Initial Configuration of Parameters for Restricted Boltzmann Machine pre-Training," *Soft Computing*, vol. 21, pp. 6471–6479, 2017.
- [17] O. Krause, A. Fischer, and C. Igel, "Population-Contrastive-Divergence: Does Consistency Help with RBM Training?," *Pattern Recognition Letters*, vol. 102, 2018.
- [18] —, "Algorithms for estimating the partition function of restricted Boltzmann machines," *Artificial Intelligence*, vol. 278, 2020.
- [19] S. Geman and D. Geman, "Stochastic Relaxation, Gibbs Distributions, and the Bayesian Restoration of Images," *IEEE Transactions on Pattern Analysis and Machine Intelligence*, vol. 6, no. 6, pp. 721–741, 1984.
- [20] P. M. Long and R. A. Servedio, "Restricted Boltzmann Machines are Hard to Approximately Evaluate or Simulate," in *International Conference on Machine Learning*, 2010, pp. 703–710.
- [21] D. M. Ceperley, "Path Integrals in the Theory of Condensed Helium," *Reviews of Modern Physics*, vol. 67, pp. 279–355, 1996.
- [22] I. Kosztin, B. Faber, and K. Schulten, "Introduction to the Diffusion Monte Carlo Method," *American Journal of Physics*, vol. 64, pp. 633–644, 1996.
- [23] A. Sarsa, K. E. Schmidt, and W. R. Magro, "A Path Integral Ground State Method," *The Journal of Chemical Physics*, vol. 113, pp. 1366–1371, 2000.
- [24] R. Srinivasan, *Importance sampling: Applications in Communications and Detection*. Springer Verlag, 2002.
- [25] D. J. Amit, *Modelling Brain Function: The World of Attractor Neural Networks*, 1st ed. New York, NY, USA: Cambridge University Press, 1989.
- [26] J. Platt, "Fast Training of Support Vector Machines using Sequential Minimal Optimization," in *Advances in Kernel Methods - Support Vector Learning*, B. Schölkopf, C. Burges, and A. Smola, Eds. MIT Press, 1999, pp. 185–208.